POST-IMPLANTATION THERMAL DESORPTION OF HELIUM FROM POLY- AND SINGLE-CRYSTALLINE IRON – Donghua Xu and Brian D. Wirth (Department of Nuclear Engineering, University of California, Berkeley, CA 94720-1730)

OBJECTIVE

The objective of this work is to experimentally measure the thermal desorption spectra of helium implanted in poly- and single-crystalline iron to determine the He trapping and diffusion kinetics. These energetic parameters are important parameters for modeling the transport and fate of He and its effect on microstructural evolution in ferritic alloy components in future fusion energy environments.

SUMMARY

The results of He desorption measurements are presented for both poly- (PC) and single-crystalline (SC) iron (>99.99%) using constant rate (1 K/s) heating following room temperature ^{4}He implantations at energies of 5 and 10 keV, and fluences of 10^{14} and 10^{15} He/cm^2. A sharp desorption peak due to BCC-FCC phase transformation is observed for both PC and SC specimens, which provides precise temperature calibration. Within the BCC structural range, three groups (I: below 300 ºC; II: 300-600 ºC; III: 600-900 ºC) of desorption signal are identified for PC specimens while only two groups (I: below 300 ºC; II: 550-900 ºC) are identified for SC specimens. The low T group appears broader for PC specimens than for SC specimens. PC and SC desorption spectra show similar dependence on implantation energy and fluence, namely that the relative intensity at low and intermediate temperatures decreases with increasing implantation energy or fluence, while the fluence effect is much more pronounced than the energy effect. Simple first order dissociation kinetics are used to estimate the average activation energies associated with all the desorption groups, and these energies range from about 1.1 to 3.4 eV. However, precise identification of the mechanisms controlling each desorption event requires further study by complementary characerization and modeling techniques. The present SC iron data are expected to provide an appropriate experimental reference for future rate-theory or kinetic Monte-Carlo modeling of helium defect evolution in BCC iron.

PROGRESS AND STATUS

Introduction

Helium effects on the microstructure and mechanical properties are among the most important subjects in fusion materials research. It has been shown that the high level of implanted or transmutationally produced (by high energy neutron flux) helium under fusion conditions can cause nucleation and growth of helium bubbles in structural materials and subsequently result in significant mechanical property degradation [1-4]. The key to understanding helium effects is to determine the mechanisms by which helium atoms migrate and interact with various microstructural features in irradiated materials. This is an inherently multi-scale problem spanning from atomistic to macroscopic dimensions in both time and space.

At the atomistic level, computer simulations using ab initio and Molecular Statics/Dynamics approaches have been performed to investigate the kinetics, energetics and thermal stabilities of He and small He-containing clusters, as well as He interactions with dislocations and grain boundaries in BCC iron [5-12]. On the nano-, micro- or macro-scopic level, experiments using optical or electron microscopy, nuclear reaction depth profiling, positron annihilation spectroscopy, coincidence Doppler broadening, thermal desorption and other techniques have been conducted to analyze He behavior and the coupled He and defect evolution in BCC iron and ferritic alloys [13-18]. More recently, continuum rate-theory modeling [19] has been compared to isothermal He desorption from BCC iron to validate ab initio results.

All previous thermal desorption experiments on iron appear to have only used poly-crystalline (PC) specimens. It is thus not clear whether the grain boundary has made any contribution to the resulting desorption signals. For the purpose of validating fundamental parameters such as migration or binding energies of He and He-V clusters, single crystalline specimens are more appropriate. In this paper we report results from thermal desorption experiments on high purity (>99.99%) specimens, which consisted of both polycrystalline (PC) and single crystal (SC) iron, following room temperature ^{4}He ion implantations at He energies of 5 and 10 keV and fluences of 10^{14} and 10^{15} He/cm^2. Similarities and distinctions

between the Helium desorption spectra for the PC and SC specimens, along with their dependence on implantation energy and fluence are presented. The desorption spectra have been analyzed using simple first order dissociation kinetics to obtain the activation energies associated with the observed desorption signals.

Experimental Procedure

High purity PC iron plates were purchased from Alfa Aesar. High purity SC iron disks were provided by Dr. S.A. Maloy at Los Alamos National Laboratory. Small specimens (~0.5-1 X 2.5 X 3.5 mm) were cut from the plates or disks, mechanically polished to 1 µm grade smoothness, and then commercially implanted at room temperature with ^{4}He ions at 5 or 10 keV to fluences of 10^{14} or 10^{15} He/cm^2. The He implantation flux was ~7-10 X 10^{10} He/cm^{2}s.

Partial He current was measured in our ultrahigh vacuum thermal desorption system (TDS) as a function of temperature during constant rate (1 K/s) ramping on each of these He-implanted specimens from room temperature up to 1300 ºC. The He current was then converted to the instantaneous desorption rate by multiplying with a proportionality coefficient, determined separately with a calibration procedure. More details regarding our TDS system are available in Reference [20].

Results and Discussion

TRIM/SRIM calculations

Probabilistic depth distributions of generated Frenkel pairs and the stopped ^{4}He ions during implantation in iron were evaluated using SRIM 2003 software [21]. For 5 and 10 keV implantation energies, the maximum production of Frenkel pairs occurs at ~12 and 26 nm below the implantation surface, while the maximum in the distribution of He occurs at 25 and 50 nm, respectively. On the average, 20 and 33 Frenkel pairs are generated per He ion for the two energies, respectively. These values correspond to a peak displacement damage of ~85 and 75 mdpa, and a peak He concentration of 2830 and 1760 appm for the two energies, respectively, at a fluence of 10^{15} He/cm^2.

Background signal

In an earlier publication [20], we noted the possibility of spurious background signal interfering with real desorption spectra and causing problems in data analysis. It is thus very critical to have a clean background in order to obtain reliable desorption data. By enhancing the cooling of the chamber walls, the problem of spurious background signal has been solved. The background He current from non-implanted control specimens now remains almost constant at a low value of ~6 X 10^{-13} A from room temperature up to 1300 ºC. In addition, the total pressure of our system is now also very low (~1X10^{-9} Torr) and stable over the entire temperature range.

General features of PC spectra and effects of implantation energy and fluence

The He desorption spectra obtained in PC specimens for the four combinations of implantation energies and fluences used in this work are presented in Fig. 1 (a)-(d). Two general features of the desorption spectra can be noticed from Fig. 1. First, there exists a sharp peak for each of the spectra around 900 ºC which is not consistent with a first order dissociation model generally adopted in classical rate theory, due to its excessive sharpness. Such a sharp peak has also been observed for PC iron and ferritic alloys under other implantation conditions [17, 20]. In Ref. [20], we discussed the strong evidence leading to the conclusion that this peak is primarily due to the alpha-gamma (BCC-FCC) phase transformation [22]. Therefore, in this work, we have used this peak to calibrate our thermocouple temperature readings by setting the peak position to 912 ºC (the well known value for alpha-gamma transformation in iron) and using a linear-correction to the other temperature values. It should be pointed out that the exact mechanism of the sharp He release peak at the alpha-gamma phase transformation is not entirely clear. Sugano et al. [17] interpreted this sharp peak as evidence for the lower stability of He-vacancy clusters in FCC iron than in BCC iron. This argument, nevertheless, can not explain the re-appearance of the peak during cooling as reported in Ref. [20], since in that case the specimen transforms back from FCC to BCC structure. Here we tend to consider this peak as a result of the transient structural instability during the proceeding phase transformation (in either direction), and that it may not represent the relative stability of

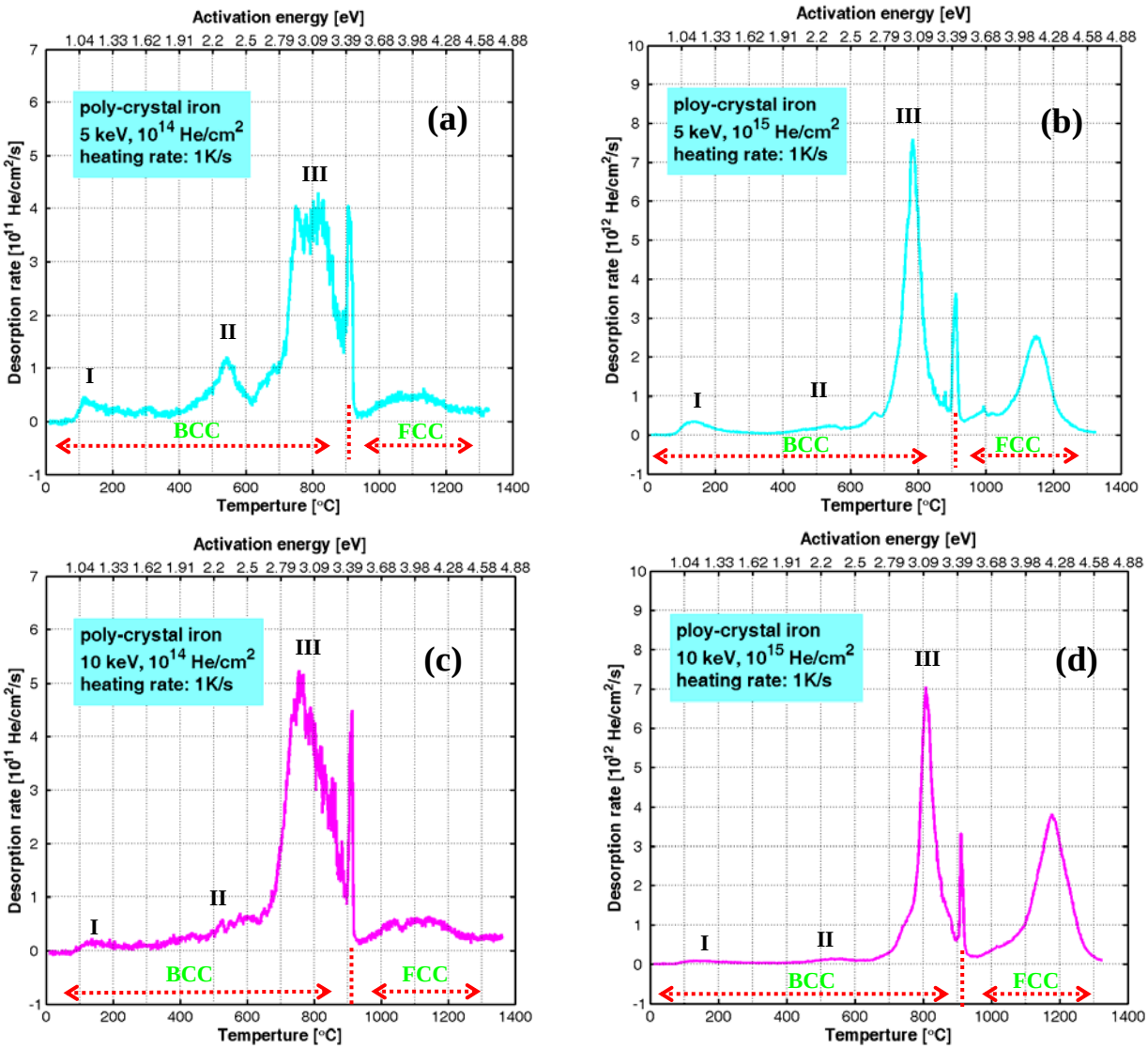

Fig. 1. Desorption spectra of high purity polycrystalline iron implanted with ^{4}He at: (a). 5 keV, 10^{14} He/cm^2; (b). 5 keV, 10^{15} He/cm^2; (c). 10 keV, 10^{14} He/cm^2; (d). 10 keV, 10^{15} He/cm^2.

He-vacancy clusters in BCC and FCC structures.

The second general feature of the observed He desorption in PC specimens is that the release signal can be divided into three groups within the BCC structural range (prior to alpha-gamma phase transformation), as shown in Fig. 1 (a)-(d). Group I lies on the low T side, spanning from room temperature up to around 300 ºC, Group II in the intermediate T range, from 300 ºC to 600 ºC, and Group III in the high T range, from 600 ºC to ~900 ºC ending with the sharp peak induced by the alpha-gamma phase transformation. Above 912 ºC, i.e., in the FCC structural range, there is another group of release signal which will be called FCC Group in the subsequent context. Here the word 'Group' is used instead of 'Peak' because each 'group' requires more than a single (defined by a definite activation energy) dissociation event to reasonably reproduce the peak width and thus, may involve multiple dissociation mechanisms [23].

By comparing the four release spectra from the PC specimens, the effect of varying implantation energy and fluence can be extracted. For example, at a fixed energy of 5 keV, as the He fluence increases from 10^{14} (Fig. 1 (a)) to 10^{15} (Fig. 1 (b)) He/cm^2, the relative strengths (intensities) of Group I and Group II at low and intermediate T with respect to the entire spectrum apparently decrease while that of the release

in the FCC phase at very high T apparently increases. Similar trends can be recognized when spectra corresponding to a common He fluence, but with increasing implantation energies are compared. However, it is evident from Fig. 1 (a)-(d) that the effect of varying He fluence is much more significant than that of varying He energy, at least within the range of fluence and energy in the present study.

General features of SC spectra – similarities and distinctions with respect to PC spectra

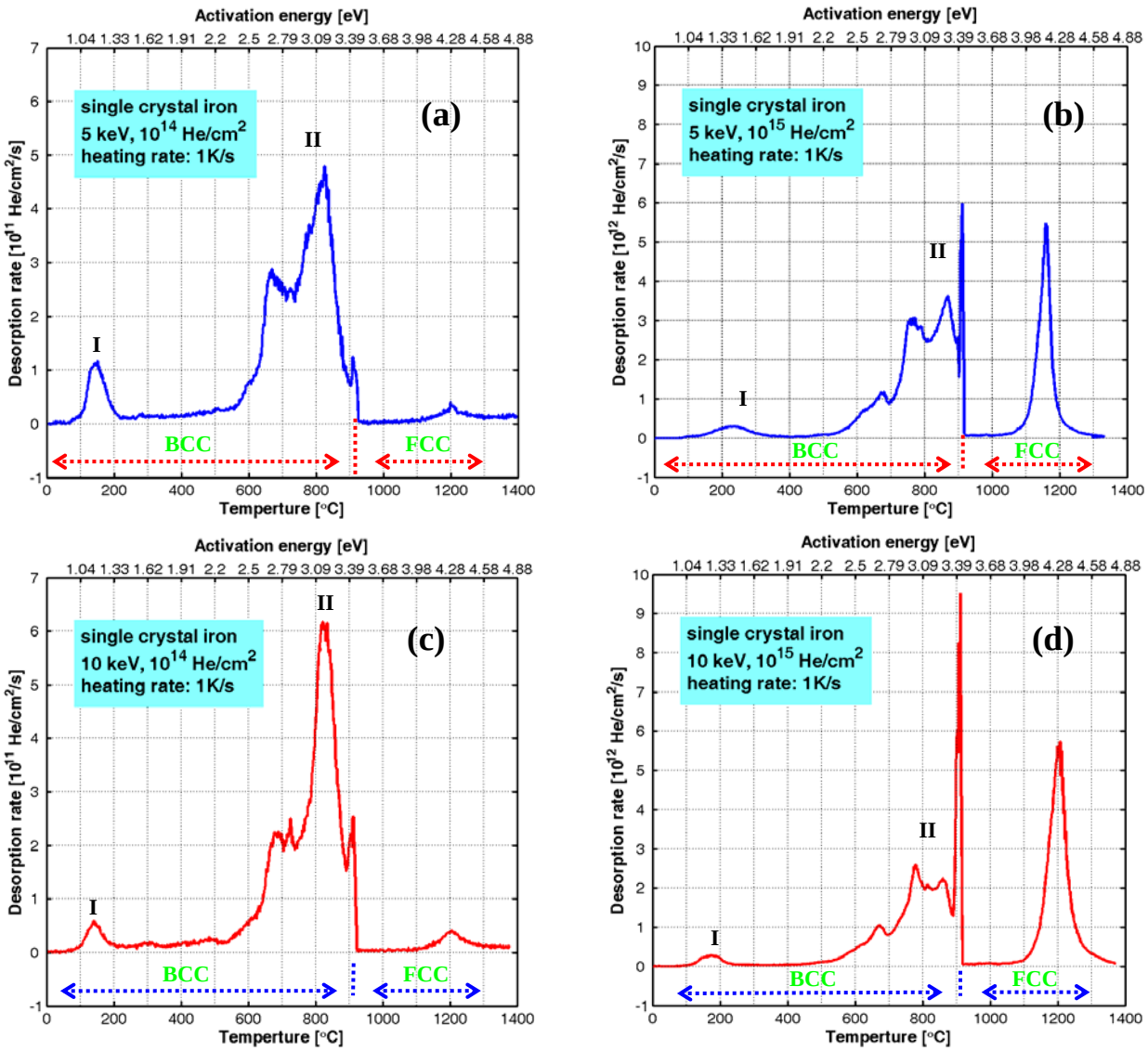

Fig. 2. Desorption spectra of high purity single-crystalline iron implanted with ^{4}He at: (a). 5 keV, 10^{14} He/cm^2; (b). 5 keV, 10^{15} He/cm^2; (c). 10 keV, 10^{14} He/cm^2; (d). 10 keV, 10^{15} He/cm^2.

As shown in Fig. 2 (a)-(d), the He desorption spectra from the SC specimens display certain similarities and distinctions when compared with the PC spectra shown in Fig. 1 (a)-(d). Similar to the PC spectra, the SC spectra also exhibit the sharp, alpha-gamma phase transformation peak, and again this peak has been used to calibrate the temperature readings. The second similarity involves the existence of multiple He release groups in well separated temperature ranges, although there are differences in the details of such grouping. Third, the SC spectra exhibit similar effects of implantation energy and fluence as the PC spectra.

The SC spectra are distinct from the PC spectra in the following three aspects. First, the SC spectra only comprise two groups of signal within the BCC structural range, Group I from room temperature to 300 ºC, Group II from ~550 ºC to 900 ºC, with no obvious signal between 300 ºC and 550 to 600ºC as in the PC spectra (Group II, PC). Second, Group I at low T and the release within the FCC phase at very high T are both narrower in SC than in PC. Third, the major desorption group (Group III for PC, Group II for SC) appears to have more splitting, or fine-scale structure in the SC specimens than in PC. The above three aspects, when viewed together, are actually consistent in that they reflect a common distinction between SC and PC spectra: SC spectra are less diffuse than PC spectra.

It is tempting to ascribe the less diffuse character of SC spectra to the absence of grain boundaries, considering the wide range of He trapping strength (binding energies) that can be provided by grain boundaries of different structures, associated with the trapping of He with excess volume in the boundary [12]. To uncover the exact reason behind the observed distinction(s) between SC and PC desorption spectra requires further investigations perhaps incorporating more systematic modification of grain boundary density. Yet, the present result evidently shows that the desorption behavior of iron is indeed influenced by the presence or absence of grain boundaries and thus that caution should be taken when comparing rate-theory or kinetic Monte-Carlo modeling results with experimental data collected from PC specimens. As a matter of fact, the present SC spectra are expected to provide additional, and perhaps more appropriate experimental reference for future modeling work.

Activation energies

In both Fig. 1 and Fig. 2, we have included an energy scale as the top axis, in correlation with the bottom temperature scale. The displayed energy values were calculated based on simple first-order dissociation kinetics, i.e., $\frac{d}{dt}N = -Nf\exp\left(-\frac{E}{k_B T}\right)$, where N is the remaining number of He atoms not yet desorbed in a specific trap, f is the jumping frequency (assumed to be 10^{13} /s), E is the activation energy for the trap, and $k_B T$ has its normal meaning. Within this model, it is straightforward to derive the relationship among peak temperature T_p, heating rate R, and activation energy E, i.e., $\ln(R/T_p^{\,2}) = -E/k_B T_p + \ln(f\ k_B/E)$ [20], which provides a one to one correlation between peak temperature and activation energy at chosen R (here 1 K/s) and f values. It should be noted that this simple model has assumed that there are no mutual transformations among traps with different E values, which is certainly not the real case since evolution among different traps/defect-clusters with distinct E values is unavoidable. However, this simple model can provide an estimate for the average E values of a group of traps which have mutual transformation among themselves and yet sufficiently separated from other groups with respect to E values.

CONCLUSIONS

In this report, we present the results of He desorption in polycrystalline and single-crystalline iron (99.99%) using constant rate (1 K/s) heating following ^{4}He implantations at energies of 5 or 10 keV and fluences of 10^{14} or 10^{15} He/cm^2. The results reveal both similarities and distinctions between the He desorption of the PC and SC specimens. The similarities include the appearance of a sharp release peak induced by alpha-gamma phase transformation, the existence of multiple desorption groups, and the influence of varying implantation energy and fluence on desorption behavior. The primary distinction is that SC spectra are less diffuse than PC spectra, which is reflected in three details: 1. within BCC structural range, SC spectra comprise only two groups of signal (Group I, room temperature to 300 ºC; Group II 550-900 ºC) as opposed to three observed in PC spectra (Group I, room temperature to 300 ºC; Group II, 300-600 ºC; Group III 600-900 ºC); 2. Group I appears narrower for SC than for PC; 3. Group II of SC display more fine-scale structure than Group III of PC. The average activation energies associated with the observed desorption groups have been estimated based on simple first order dissociation kinetics. While the underlying microscopic mechanisms are not entirely clear at this stage, our result suggests that it may not be advisable to compare rate-theory or kinetic Monte-Carlo modeling which does not include grain boundaries with desorption experiments conducted on PC specimens. The present

desorption data from SC iron are expected to provide additional, and perhaps a more appropriate experimental reference for future modeling.

ACKNOWLEDGEMENTS

The authors thank Dr. Stuart A. Maloy (LANL) for providing the single crystal Fe specimens, and Drs. Maria Jose Caturla (University of Alicante), Cu-Chun Fu (CEA-Saclay), Rick Kurtz (Pacific Northwest National Laboratory), Bob Odette (University of California, Santa Barbara), Christophe Ortiz (University of Alicante), and Kazunori Morishita (University of Kyoto) for helpful discussions. This work has been supported by the Office of Fusion Energy Sciences, U.S. Department of Energy, under Grant DE-FG02-04ER54750.

REFERENCES

[1] L.K. Mansur, and W.A. Coghlan, J. Nucl. Mater. **119**, 1 (1983).
[2] H. Ullmaier, Nucl. Fusion **24** (1984) 1039.
[3] L.K. Mansur, and M.L. Grossbeck, J. Nucl. Mater. **155**, 130 (1988).
[4] H. Trinkaus, and B.N. Singh, J. Nucl. Mater. **323** (2003), 229.
[5] K. Morishita, R. Sugano, B.D. Wirth, and T.D. de la Rubia, Nucl. Instrum. Methods Phys. Res. B **202**, 76 (2003).
[6] B.D. Wirth et al., J. Nucl. Mater. **329**, 103 (2004).
[7] C.C. Fu, and F. Willaime, Phys. Rev. B **72**, 064117 (2005).
[8] L. Ventelon, B.D. Wirth, and C. Domain, J. Nucl. Mater. **351**, 119 (2006).
[9] T. Seletskaia, Y.N. Osetsky, R.E. Stoller, and G.M. Stocks, **351**, 109 (2006).
[10] F. v.d. Berg, W. v. Heugten, L.M. Caspers, and A. v. Veen, Solid State Commu. **24**, 193 (1977).
[11] H.L. Heinisch, F. Gao, R.J. Kurtz, and E.A. Le, J. Nucl. Mater. **351**, 141 (2006).
[12] R.J. Kurtz, and H.L. Heinisch, J. Nucl. Mater. **329**, 1199 (2004).
[13] M.B. Lewis, and K. Farrell, Nucl. Instrum. Methods Phys. Res. B **16**, 163 (1986).
[14] K. Arakawa, R. Imamura, K. Ohota, and K. Ono, J. Appl. Phys. **89**, 4752 (2001).
[15] T. Ishizaki, Q. Xu, T. Yoshiie, and S. Nagata, Mater. Trans. **45**, 9 (2004).
[16] T. Iwai, Y. Ito, and M. Koshimizu, J. Nucl. Mater. **329**, 963 (2004).
[17] R. Sugano, K. Morishita, and A. Kimura, Fusion Sci. Tech. **44**, 446 (2003).
[18] R. Vassen, H. Trinkaus, and P. Jung, Phys. Rev. B **44**, 4206 (1991).
[19] C.J. Ortiz, M.J. Caturla, C.C. Fu, and F. Willaime, Phys. Rev. B **75**, 100102 (2007).
[20] D.H. Xu, T. Bus, S.C. Glade, and B.D. Wirth, J. Nucl. Mater. **367**, 483 (2007).
[21] J.F. Ziegler, J. P, Biersack, and U. Littmark, The Stopping and Range of Ions in Matter, Pergamon, New York 1984.
[22] The temperature readings in Ref. 20 are not accurate, but the analysis and qualitative conclusions are not affected.
[23] D.H. Xu, and B.D. Wirth, unpublished research.